SUPPLEMENTAL DATA

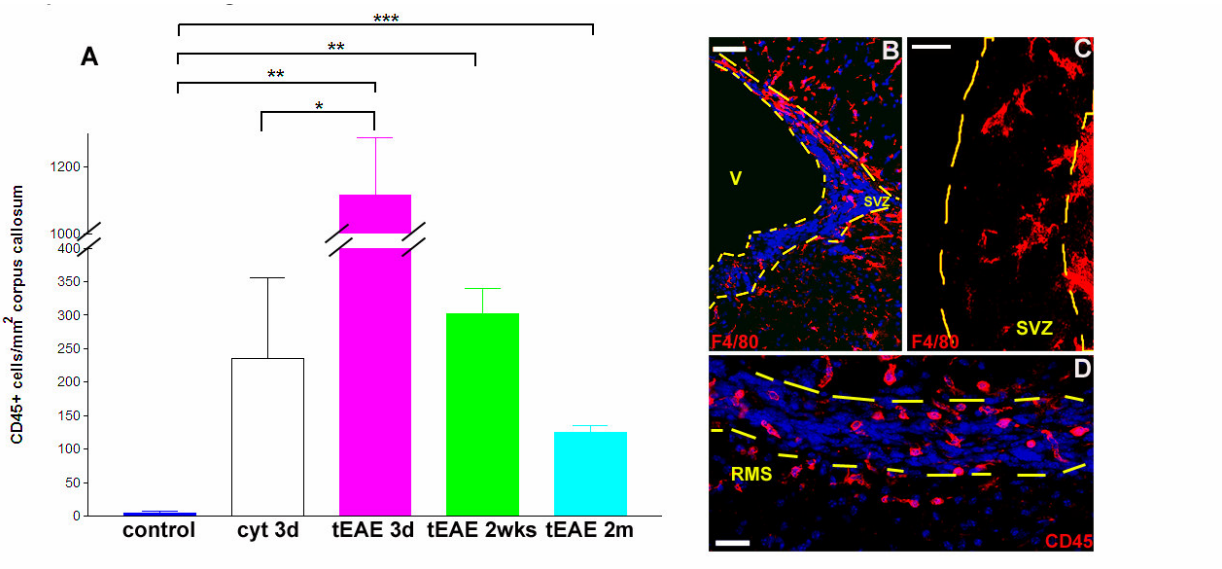

Figure S1. Inflammation in SVZ/RMS

A. Quantification of haematopoietic cells in the corpus callosum (n= 3 mice/group). A drastic increase in numbers of CD45+ cells occurs in tEAE 3 days p.i. as compared to the controls (**p=0.0029) or non-immunized mice injected with cytokines and sacrificed 3 days p.i. (*p=0.0136). Numbers of CD45+ cells remain significantly upregulated in tEAE mice sacrificed at 2 weeks and 2 months p.i. (**p=0.0015 and ***p=0.0002 respectively) as compared to the controls. **B-D.** Illustration of the inflammatory cells in the SVZ/RMS of tEAE mice. **(B.)** During the first week p.i., many cells positive for the activated microglia/macrophage marker F4/80 are present in the SVZ. **(C.)** Higher power view of F4/80+ SVZ cells acquiring ameboid form suggestive of activated microglia; **(D.)** Numerous haematopoietic cells positive for CD45 are found in the RMS during the first week p.i. Scale bars b=50 µm, c-d=25 µm.

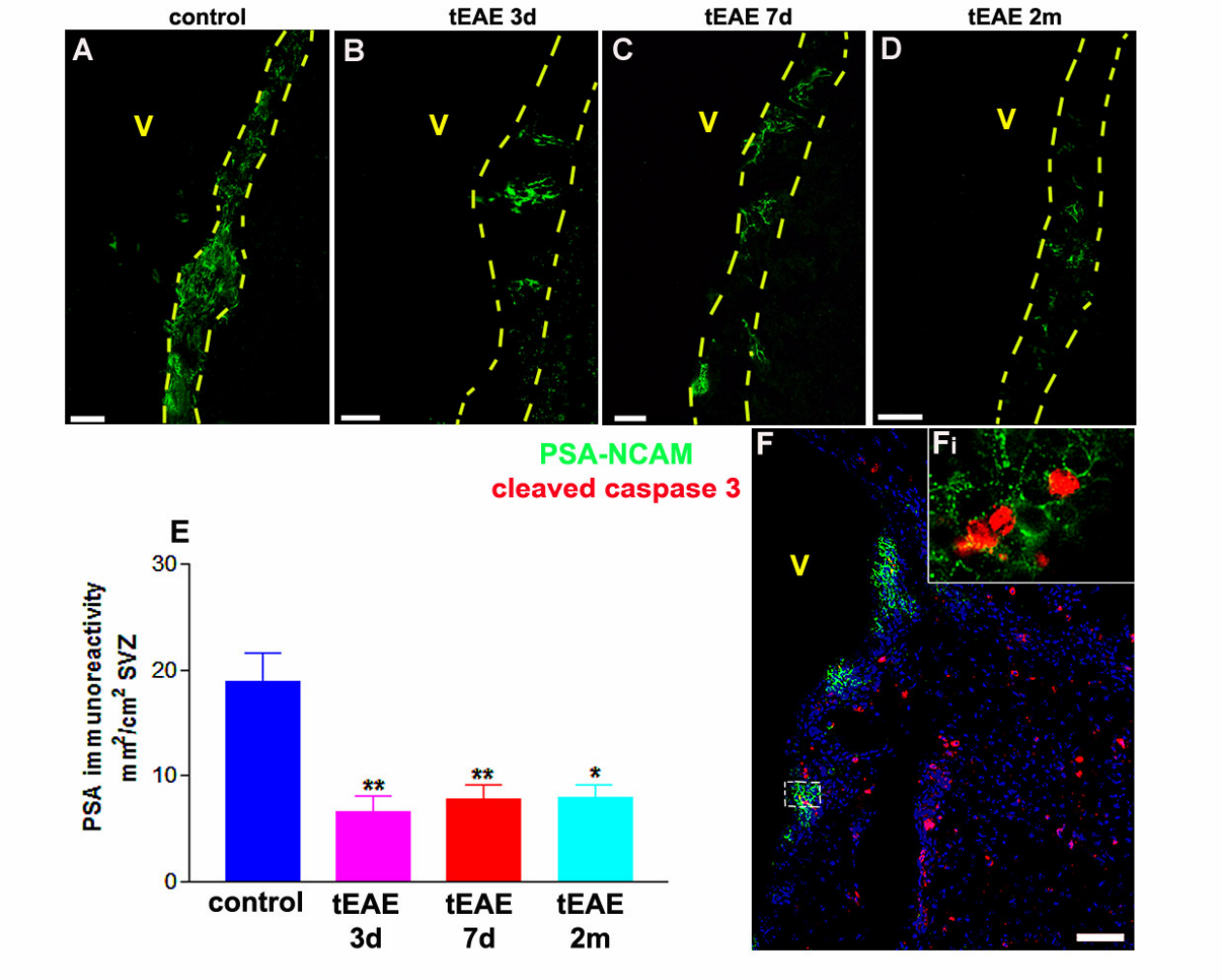

Figure S2. Reduction in PSA-NCAM positive cells in targeted EAE SVZ and evidence of early neuroblast apoptosis

A-D Representative images of SVZ area in control (**A**) and tEAE (**B-D**) mice. **A.** Numerous positive cells are present along the lateral ventricle in control tissue. **B-D.** Dispersed patches of PSA-NCAM positive cells can be found in tEAE SVZ at 3 days p.i. (**B**), 7 days p.i.(**C**), and 2 months p.i.(**D**). **E.** Quantification of PSA-NCAM immunoreactivity within SVZ represented in millimetres squared labelled area per centimetres squared SVZ area measured. A significant decrease compared to the control is obvious at 3 days, 7 days, and 2 months p.i. (**p=0.0041, **p=0.0061, and *p=0.0114 respectively; n=4-5mice/group). Error bars represent SEM. **F.** Immunohistochemistry for cleaved caspase 3. Three days p.i., some dispersed PSA-NCAM+ neuroblast patches contain cleaved caspase 3+ cells. **Fi.** Higher power view of cleaved caspase 3+ neuroblasts. Scale bars a-d=25 µm, f = 50 µm.

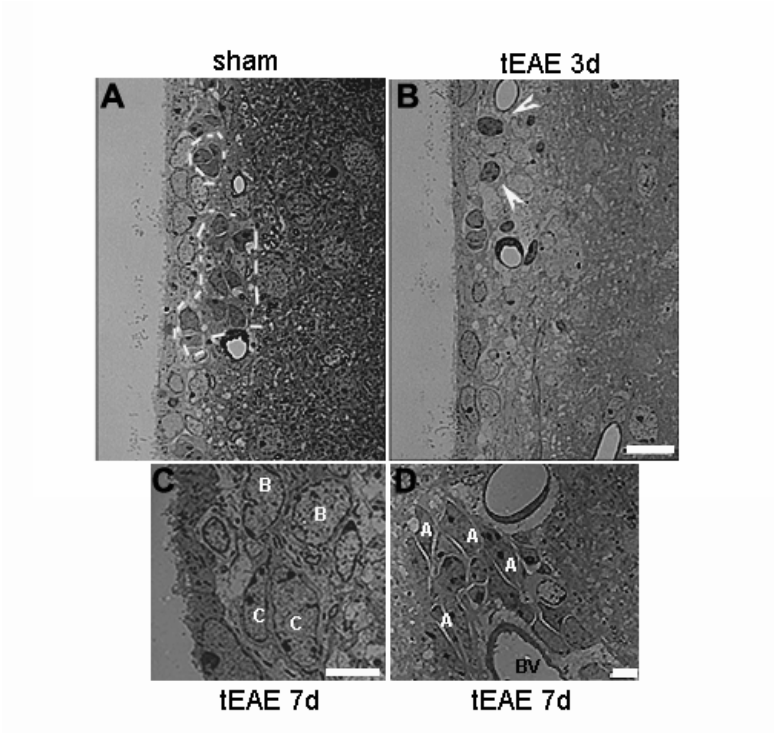

Figure S3. Ultrastructural changes in the SVZ during tEAE

A-B. Representative images of 1.5µm-thick resin sections in sham injected **(A)** and tEAE **(B)** mice 3 days p.i. **(A.)** Sham injection does not induce loss of chain migration, as numerous groups of neuroblasts are present (dark cells surrounded by white dotted lines). **(B.)** In tEAE mice, large areas free of migrating chains are observed, with few individual cells present (arrowheads). **C.** Groups of large B and C cells are present in tEAE SVZ 7 days p.i. suggesting increased activity. **D.** Large groups of neuroblasts can be found at the distance from the SVZ next to striatal blood vessels suggesting considerable emigration outside neurogenic areas at 7 days p.i.; Scale bars a-b =10µm, c= 6µm, d= 5µm.

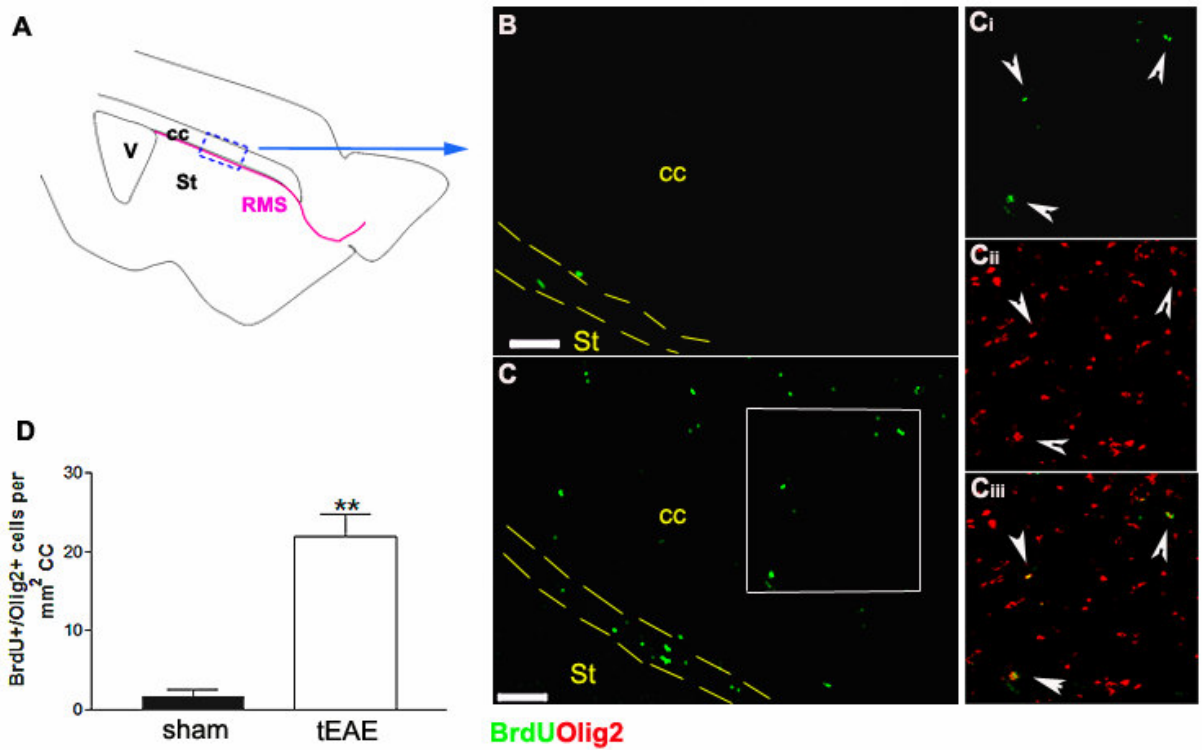

Figure S4. Targeted EAE increases numbers of SVZ-derived oligodendrocyte lineage cells in the corpus callosum.

A. Schematic representation of saggital mouse forebrain section. A rectangle delimited by blue dotted lines area illustrates the area shown in **B**-**C**. **B**-**C.** BrdU tracing of SVZ-progeny in sham (**B**) and tEAE (**C**) mice 2 weeks p.i. **(B.)** Few labelled cells are present in sham RMS, none in the corpus callosum (most cells had been found in the olfactory bulb-Fig 6). **(C.)** Lesioned corpus callosum area in tEAE mouse contains numerous BrdU+ cells (green), some of which co-label for Olig2 (red). **Ci-Ciii.** higher magnification view of boxed area in **(C)**. Scale bars= 50 µm. **D.** Quantification of BrdU+/Olig2+ cells showing numbers of positive cells per millimetre squared of corpus callosum area measured, **p=0.0022, n=3 mice/group. Error bars represent SEM.

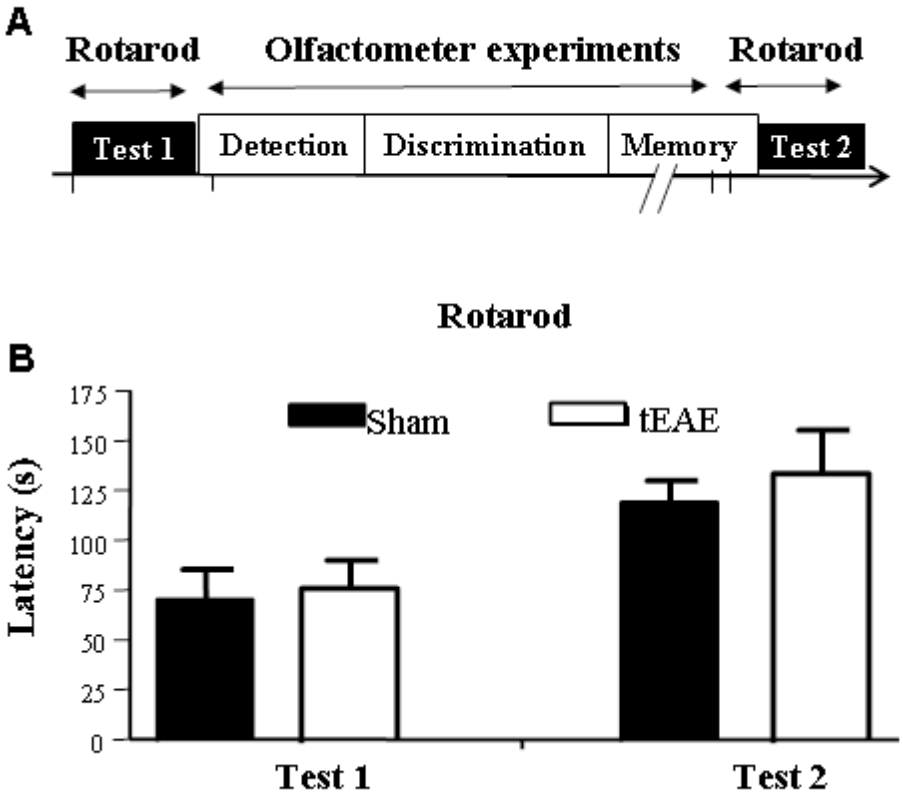

Figure S5. Motor abilities of tEAE mice used in the olfactometer experiments.

A. Two weeks after cytokine intracerebral injection, sham and tEAE mice were tested using Rotarod (day 1). Nine tEAE mice without motor dysfunction assessed by rotarod test were selected. Mice were partially water-deprived during one week and then trained to perform two-odorant discrimination tests using olfactometer. Odorant detection, discrimination and olfactory memory were investigated. At the end of olfactometer experiments, a second rotarod test was performed. **B.** Mean latency before falling for the two rotarod tests are shown for sham and tEAE mice. No difference between the groups was observed. Error bars indicate SEM.

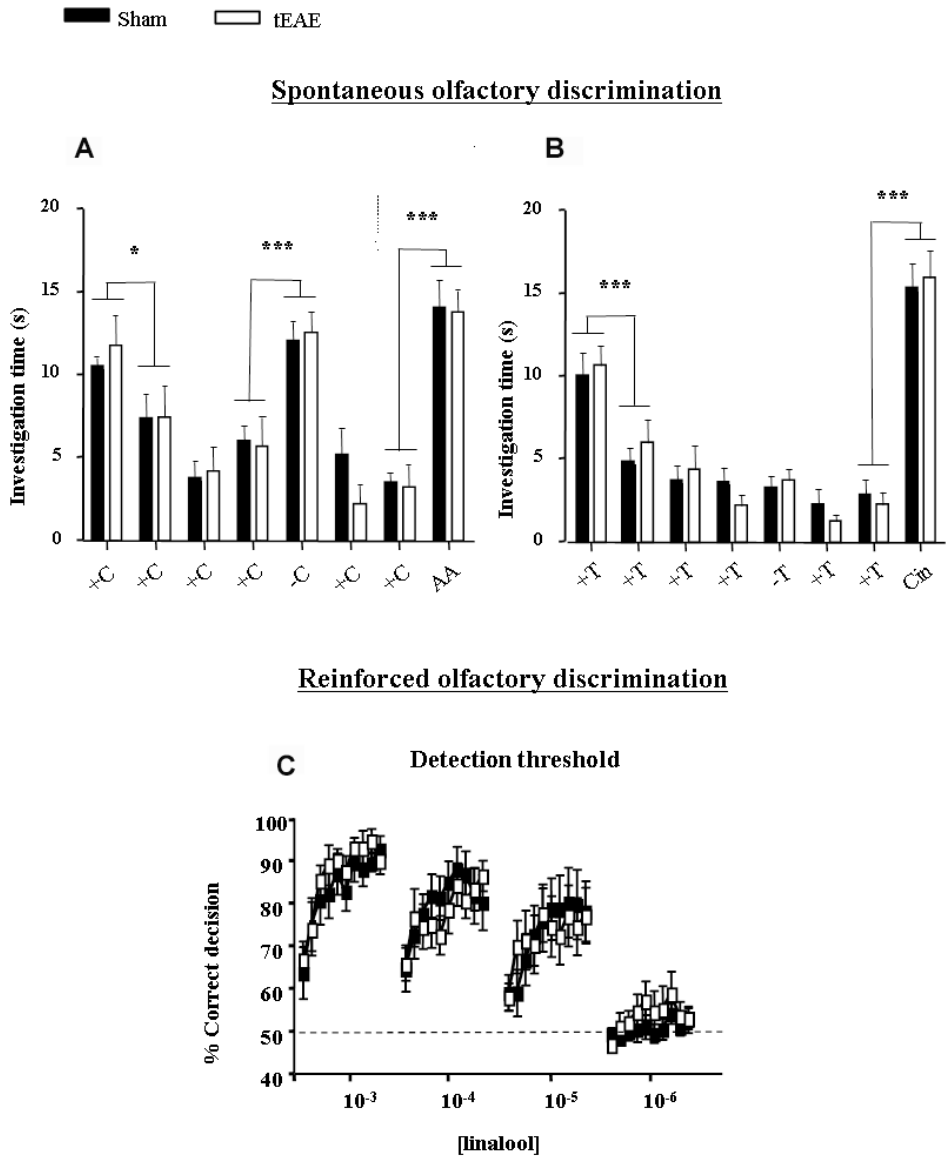

Figure S6. Olfactory discrimination in tEAE mice.

Spontaneous olfactory discrimination (A-B). **A.** Both sham and tEAE mice detect small differences between similar odorants such as Carvone (C) enantiomers. **B.** Neither tEAE nor sham mice can spontaneously distinguish between terpinen (T) enantiomers, but successfully recognize the difference between T and Cineole (Cin). (n=7-9 mice/group). **C.** Two-odorant discrimination tasks assessed by olfactometers. Accuracy (% of correct responses) is shown for detecting successively lower concentrations of linalool (10 blocks of 20 trials). Linalool (L) served as the rewarded (S+) stimulus and the mineral oil (MO) as the non-rewarded (S-) stimulus. First, water-deprived mice were trained to distinguish between high concentrations of L and MO and then exposed daily to progressively lower concentrations. A score of 50 % represents the level expected to be obtained by chance alone (dashed line). No differences were observed for tEAE mice compared to sham. n=7-9 mice/group.

	Control	t EAE 3d	t EAE 7d	t EAE 1m	t EAE 2m
Total cells	138 ± 13.42	119.7 ± 7.99	136 ± 8.13	119 ± 13.05	98 ± 6.342
Ependymal cells	32.15± 2.9	37.89 ± 3.43	35.2 ± 2.59	35.03 ± 1.79	23.69 ± 2.12
Astrocytes	33.75 ± 6.19	38.18 ± 0.9	40.95 ± 2.40	33.44 ± 3.52	26.2 ± 2.09
Astrocytes contacting lateral ventricle	1.05 ± 0.54	0.21 ± 0.21	0.54 ± 0.43	0.14 ± 0.07	0
Neuroblasts	43.14 ± 2.62	18.52 ± 3.27	30.08 ± 8.26	21.96 ± 5.43	18.02 ± 5.09
Type C cells	15.91 ± 2.46	14.24 ± 5.35	20.54 ± 1.18	20.74 ± 4.81	25.38 ± 6.13
Mitotic features	0.75±0.06	0.21±0.21	0.66±0.28	0.68±0.12	0.39±0.22
Pyknotic cells	0.37 ± 0.19	1.13 ± 0.08	0.32 ± 0.2	0.37 ± 0.2	0.14 ± 0.14
Microglia	1.02 ± 0.19	4.35 ± 1.36	4.81 ± 1.67	1.69 ± 0.33	2.46 ± 1.22
Neurons	1.157 ± 0.44	1.63 ± 0.67	1.68 ± 0.63	2.08 ± 0.19	1.62 ± 0.4

Table S1. Ultrastructural characterization of different cell types within the ventricular wall and subependymal area in control and targeted EAE mice.

Values presented show cell number/millimetre SVZ length ± SEM; n=3-4 mice/group.

Case	Sex	Age (years)	PMD (h)	Disease duration (years)	Cause of death	Course	Lesions			
							Active lesion	Chronic active lesion	Chronic silent	Shadow plaques
MS100	M	46	7	8	Pneumonia	SP		1		1
MS107	M	38	19	16	Aspiration pneumonia, pulmonary oedema	RP		1	1	
MS54C4	F	69	11	31	Pneumonia	SP		1		
MS54C5	F	69	11	31	Pneumonia	SP	1	1		
Non neurological controls:										
C05	F	95	10		bronchiopneumonia old age (as per death certificate)					
C19	F	90	15							

Table S2. Clinical data of the MS cases used in the study.

PMD, postmortem delay; SP, secondary progressive; RP, relapsing progressive

EXPERIMENTAL PROCEDURES

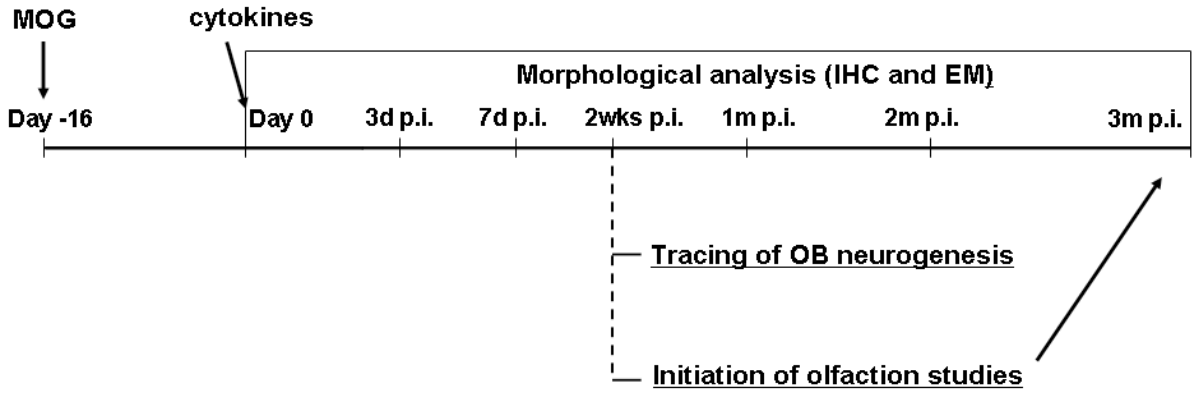

Experimental outline chart of tEAE induction and summary of different analyses performed at various survival times

Rotarod test

This test measures the ability of an animal to maintain balance on a rotating 4.5 cm diameter rod (Bioseb). This task reflects motor ability and coordination. Mice were subjected to 3 trials separated by 10 min-intervals during which rotation speed increases from 4 to 40 rpm in 5 min. The latency to fall off is recorded and the mean latency calculated for each mouse.

RESULTS

Clinical signs development in a minority of tEAE mice

Development of clinical deficits in tEAE mice was variable between different experimental sets. While on cytokine injection day none of the mice presented clinical EAE signs, starting at 2 weeks p.i. 5-10% of mice in certain experimental sets developed clinical EAE signs of variable extent (not shown). Immunohistochemical analyses showed presence of

inflammatory spinal cord lesions in these mice but no difference in the presence/extent of brain inflammation. For morphological analyses of the SVZ, only mice that developed deficits less than a week before sacrifice at late time points (2 months) were used and no quantitative difference was observed between these and non-affected EAE mice suggesting that forebrain inflammation/demyelination rather than spinal cord pathology induced SVZ changes.

Targeted EAE mice are clinically apt for olfactory tests

For functional studies, we first examined whether tEAE mice suffered clinical deficits that would render them unfit for the olfaction tests. While no changes in locomotor activity (using actimeter during 24h) nor in anxiety levels (light/dark test during 10 min; not shown) occurred, we detected minor motor deficits in about 25% tEAE mice compared to sham mice using a rotarod test (not shown). Thus we took into account whether the mouse exhibited or not motor deficits to assign it to different cohorts of tEAE mice: For spontaneous paradigms, we used both cohorts of sham and tEAE mice. For operant conditioning paradigms where motor abilities may be more important for performance, we only used those sham and tEAE mice without motor deficit in the rotarod test (Figure S5). All selected tEAE mice used for operant conditioning paradigms presented a significant deficit in DCX+ neuron number in the OB at the end of behavioral experiments (Figure 6G-H,L).

Olfactory discrimination and short-term olfactory memory are unaffected in tEAE mice

Targeted EAE and sham mice were first subjected to a spontaneous olfactory discrimination task (Figure 8A, Figure S6A-B). The two groups of mice discriminated well between dissimilar and moderately similar odorants (Figure 8A, Figure S6A) but failed to spontaneously distinguish between very similar odorants (Figure S6B). Thus, these findings show that

spontaneous olfactory discrimination of high concentrations of odorants was not altered by tEAE inflammation.

The ability of tEAE and sham mice to detect very small changes in odorant concentrations was tested using an automated operant conditioning procedure, a go out test, with two-odorant rewarded discrimination task. Threshold for linalol detection, acquisition rates and degrees of success were identical for both groups of mice (Figure S6C). In addition, the two groups of mice discriminated similarly between mixtures of odorants consisting in varying linalool/mineral oil ratio (Figure 8B). These results therefore demonstrate that tEAE inflammation spares the ability to successfully complete difficult olfactory discrimination tasks.

To assess short-term olfactory memory, mice were exposed twice to mint odorant (habituation), and re-exposed to the same odorant after a 30 min interval (Figure 8C). No difference in investigation time spent during the second and third exposure periods was detected (Figure 8D), suggesting that the inflammation-induced deficit in the neuronal supply to the OB had no effect on spontaneous short-term memory.